Fire Technology, 53, 577–607, 2017

Manufactured in The United States
DOI: 10.1007/s10694-016-0632-0

# EcoSmart Fire as Structure Ignition Model in Wildland Urban Interface: Predictions and Validations

*Mark A. Dietenberger* and Charles R. Boardman, Forest Products Laboratory, USDA, FS, Madison, WI 53726, USA*

**Received:** 30 September 2015/**Accepted:** 25 October 2016

***Abstract.*** EcoSmartFire is a Windows program that models heat damage and piloted ignition of structures from radiant exposure to discrete landscaped tree fires. It calculates the radiant heat transfer from cylindrical shaped fires to the walls and roof of the structure while accounting for radiation shadowing, attenuation, and ground reflections. Tests of litter burn, a 0.6 m diameter fire up to 250 kW heat release under a Heat Release Rate (HRR) hood, with Schmidt-Boelter heat flux sensors in the mockup wall receiving up to 5 kW/m$^2$ radiant flux, in conjunction with Fire Dynamic Simulator (FDS) modeling verified a 30% radiant fraction, but indicated the need for a new empirical model of flame extinction coefficient and radiation temperature as function of fire diameter and heat release rate for use in ecoSmartFire. The radiant fluxes predicted with both ecoSmartFire and FDS agreed with SB heat flux sensors to within a few percent errors during litter fire growth. Further experimental work done with propane flame heating (also with 30% radiant fraction) on vertical redwood boards instrumented with embedded thermocouples validated the predicted temperature response to within 20% error for both models. The final empirical correlation for flame extinction coefficient and temperature is valid for fire diameters between 0.2 and 7.9 m, with heat release rates up to 1000 kW. From the corrected radiant flux the program calculates surface temperatures for a given burn time (typically 30 s) and weather conditions (typically dry, windy, and warm for website application) for field applications of many trees and many structural surfaces. An example was provided for a simple house exposed to 4 burning trees selected on a Google enhanced mapping that showed ignition of a building redwood siding. These temperatures were compared to damage or ignition temperatures with output of the percentage of each cladding surface that is damaged or ignited, which a homeowner or a landscaper can use to optimize vegetation landscaping in conjunction with house exterior cladding selections. The need for such physics-based fire modeling of tree spacing was indicated in NFPA 1144 for home ignitability in wildland urban interface, whereas no other model is known to provide such capability.

**Keywords:** Wildland-urban interface fires, Structure ignition modeling, ecoSmart landscape, Building and vegetation clearances, Critical radiant fluxes, Building piloted ignition

* Correspondence should be addressed to: Mark A. Dietenberger, E-mail: mdietenberger@fs.fed.us

**Nomenclature**

| | |
|---|---|
| $A$ | Surface area ($m^2$) |
| $Bi$ | Biot number |
| $D$ | Tree flame diameter (ft (m)) |
| $c$ | Heat capacity (J $kg^{-1}$ $K^{-1}$) |
| $\delta_m$ | Cladding thickness (mm) |
| $\varepsilon_m$ | Tree flame emissivity (–) |
| $E_b$ | Blackbody total emissive flux ($kWm^{-2}$) |
| $F_i$ | Cylindrical flame view factor in "I" direction (–) |
| $Fo$ | Fourier number (–) |
| $Fr$ | Froude number based on heat release rate (–) |
| $h$ | Heat transfer coefficient (W $m^{-2}$ $K^{-1}$) |
| $H$ | Tree flame height (ft (m)) |
| $HRR$ | Heat release rate of tree (kW) |
| $k$ | Thermal conductivity ($Wm^{-1}$ $K^{-1}$) |
| $\kappa$ | Smoke extinction coefficient ($m^{-1}$) |
| $L$ | Distance from surface element to flame center (m) |
| $m$ | Tree wet mass (kg) |
| $MC$ | Dry basis moisture content of tree foliage (%) |
| $q_j$ | Line of sight irradiance from tree fire j to surface element ($kWm^{-2}$) |
| $\rho$ | Cladding density (kg $m^{-3}$) |
| $r$ | Flame radius (m) |
| $R_j$ | Ground reflection coefficient around tree j (–) |
| $S_j$ | Mean beam length of tree fire j (m) |
| $\sigma$ | Stefan-Boltzmann constant, ($5.6696 \times 10^{-8} \times Wm^{-2} K^{-4}$) |
| $\tau_j$ | Tree flame transmittance (–) |
| $\theta_0$ | Upward rotation angle to flame top (radian) |
| $T$ | Temperature (K) |
| $u$ | Unit vector in $x$ direction of element normal vector |
| $v$ | Unit vector in $y$ direction of element normal vector |
| $w$ | Unit vector in $z$ direction of element normal vector |
| $\chi_r$ | Radiant fraction of heat release rate |

# 1. Introduction

EcoSmartFire is part of a suite of software tools designed to help evaluate the environmental impact of landscaped outdoor spaces (www.ecosmartlandscapes.org), known as ecoSmart Landscapes. This fire component implements a flexible PC-based fire model on a web-based server that helps to estimate the fire hazard to a structure from nearby individualized trees, thus responding to the need for tools which promote reduced home ignitability in the wildland-urban interface (NFPA 1144) [1]. The principal ignition sources for a structure are: flame radiation assisted with piloted ignition by small aerial embers, flame impingement particularly that promoted by convection, and accumulated firebrands as described by Cohen [2]. Firebrands are burning embers from vegetation or other burning materials within the structure ignition zone of 30 to 60 meters [3] from the home that undergo aerial transport by winds and fire-driven currents which can end up at an accumulation point on the structure or the landscaped vegetation and mulch on the property. Firewise [4], Nader, et al. [5], and the ICC WUI Code [6] similarly describe the home ignition zone within the first 60 m (200 ft) of a home. EcoSmartFire addresses the fire hazard from flame radiation and assumes the other hazards are accounted for by hardening the home.

Although the survivability of a home within the wildland-urban Interface depends on a number of factors, the most important is preventing ignition on important exterior components as noted by Babrauskas [7] and by Ellis and Sullivan [8]. The desire to prevent structural ignition has resulted in various recommendations as reported in the literature based primarily on anecdotal knowledge. For example, the case study of the Bel Air fire [9] by Howard reported home ignition based on home characteristics and their surroundings in which 95 percent survival was achieved for homes with noncombustible roofs and a vegetation clearance of 10 to 18 meters. Another case study of the Painted Cave fire [10] by Foote indicated 86 percent survival for homes with noncombustible roofs and a clearance of 10 meters or more of vegetation. Researchers have obtained some additional clarity with testing and fire modeling. For example the Structure Ignition Assessment Model (SIAM) was developed at USDA Forest Service—Forest Products Laboratory (FPL) by Tran and others [11] in collaboration with Cohen in the 1980s. SIAM was limited by a simplified flux time procedure calibrated for wood siding materials and for the worst case radiant exposure to extreme crown wildfire. Based on SIAM results recommendations were made that the forest fireline should be conservatively no closer than about 10 to 40 meters from any combustible structure [2]. SIAM does not consider exposure to ornamental vegetation fires and is unable to provide specific landscaping recommendations or structural modification recommendations to the homeowner. EcoSmartFire was created to improve these recommendations.

To be able to relax the previous restrictions the firebrand hazard must be addressed. Field and large-scale observations have been placing greater emphasis on the firebrands as causing the home losses [12 and other papers in this issue]. The firebrands can penetrate soffit vents or accumulate in crevices around the home, or pile up on the ground or decks below combustible vertical claddings, or pass through broken windows. Thus additional fire resistance to the home beyond that of Class A roofs (UL 790) to address the firebrand problem is being promoted [1, 9, 10]. Also being promoted is the stay and defend strategy [13] in which after the wildfire passes by, the inhabitants of a fire resistive home put out any spot fire started by the firebrands. Realizing the importance of firebrands and ladder fuel [4–6, 12], the ornamental vegetation is cautiously reintroduced on the parcel by choosing fire resistant species, effective landscaping, and eliminating ladder fuels that promote crown fire or ground fire spread. Indeed, the California Public Resources Code 4291 requires the removal and clearance of all flammable vegetation and other combustible growth within 9 m (30 ft) of the house, but allows single specimens of trees, shrubs, or other vegetation provided that they are well spaced and well pruned. Although mulch is described also as a threatening fuel [14], its impact is considerably reduced by following NFPA 1144 [1] or Firewise [4] for removal of adjoining combustibles to avoid flame contact with the house. However, once the firebrand threat becomes mitigated with effective structural hardening, one can argue that even greater leniency can be provided for ornamental vegetation and landscaping and reduce the need for defensible space, particularly if soil moisture management, energy savings via shading, carbon content, and aesthetics are desirable features [15]. Hence the need arises to provide the homeowner or landscaper a tool for scientifically based selections of ornamental vegetation and structural protection claddings, without introducing the complexity of computational fluid dynamics code such as the Fire Dynamic Simulator.

The EcoSmartFire software provides such a physics-based model by calculating the tree flame radiation source along with piloted ignition and heat damage for structural response, estimating the hazard to the structure from the placement of trees on the property, and thus promoting placement at sufficient distance and shading to reduce risk if all the trees within the immediate landscape area became involved in crown fires simultaneously from an intense wildfire and with finite burn time duration. There is still the need to address the flame impingement risk through removal of combustible materials adjacent the structure, and hardening the structure against firebrand risk through use of Class A roofing, appropriately constructed walls, windows, and doors, and vent blockage methods. NFPA 1144 [1] addresses these required remedies, while it specifies that, "6.2.5 Tree crowns within the structure ignition zone shall be spaced to prevent structure ignition from radiant heat". The ICC WUI code [6] can be consulted for similar recommendations. No calculation was provided nor recommended for this tree crown spacing recommendation, and it appeared that anecdotal knowledge was only available to suggest spacing of 3 m (10 ft) between trees. EcoSmartFire can provide that calculation by improving on previous flame radiation calculations in the 2008 Society of Fire Protection Engineer (SFPE) Handbook of Fire Protection Engineering and other selected publications cited in this paper through use of an improved radiation heat transfer model, as developed and validated in this work, and the use of critical surface temperatures for damage and ignition on the exposed surface. Since damaging temperatures on these components are typically much lower than the piloted ignition temperatures, efforts to minimize heat related damage will also result in conservative structural protection from ignition. This conservative evaluation on the basis of damage instead of ignition will tend to compensate for physical attributes not modeled in ecoSmartFire such as windblown leaning of flames toward the house, or of ground combustion. This approach generalizes the critical heat flux criterion that is based on a very long heat exposure time typical of adjacent fires on combustible buildings. The model assumes a special exception for the Class A combustible roofing, in that piloted ignition temperature can be exceeded locally, and yet the fire remains localized and self-extinguishes once the heat source diminishes or is removed. Such a roof could be considered as only damaged, and not as sustained ignition. Exceptions on other structural components similar to the Class A roofing can be developed as testing protocols continue to be improved for them.

EcoSmartFire software runs on a web server along with other components of the ecoSmart Landscape. It relies on the web software for user input that defines the landscape and building, and web tools for user output to convey the risk to each building surface. Internally it reads in a text based file at a known location on a hard drive and outputs a text file with its calculated results for each surface. Thus the software can be run on any Windows based machine for testing and validation of the fire model, while also running in the multiuser environment of a web server. However, keep in mind that its use in the web server limits the structure to 4 walls and 1 roof, and up to 9 arbitrary trees on the property to limit computation time, whereas on the PC many structural surfaces with many trees on the lot can be used as the computation time is much less limiting. This manuscript documents the core fire model, validation with fire tests under the Heat Release Rate (HRR) hood, and some examples of model predictions with ecoSmart Landscape and with specific scenarios involving selection of building claddings.

## 2. Understanding Core Fire Model—FireModel Overview

EcoSmartFire software runs on the Windows hardware platform. The input file contains information about the location of the walls and roof, along with surface material properties. It also includes the tree location and other tree properties needed to calculate the heat release rate of the trees. The output file contains percentage of each surface damaged and ignited by the heat flux, and the heat release rate and burn time of each tree. Each input wall and tree is numbered and the output file contains information for the corresponding wall or tree. Full details of various routines will be provided in a FPL General Technical Report after this publication, while some basic information on program structure is provided in this section.

The FireModel subroutine does most of the work. After validating the location and outward normal vector for all structural surfaces, and calculating the heat release rate profile of the trees, it runs the CalcDamage function for each surface. CalcDamage breaks up the surface into many small elements and calculates the heat flux and exposure time from all burning trees to each surface element. Then it uses surface material properties and fixed atmospheric condition to predict surface temperature rise for each element, and compares the predicted temperature to the critical temperatures for damage and ignition (see Table 1). Finally it stores the percentage of damaged or ignited elements for output.

The core flame thermal radiation calculations are done inside the CoreFlux subroutine which is called by CalcDamage. It takes a particular surface element, and sums the contribution to temperature rise from the heat flux profile of all trees. The heat flux calculation is based on the direct line-of-sight radiative heat transfer from a cylindrical shaped fire in the tree crown to the surface element in question, while adjusting for the blocking of that line of sight from other trees and other parts of the structure, and including ground reflections of the radiative heat flux. The formulae for flame characteristics of burning trees and the radiative heat transfer to differential surfaces are taken from the SFPE Handbook of Fire Protection Engineering [16]. Early experimental work attempting to validate these formulae resulted in modifications to flame temperature and emissivity. Further, as there are numerous trees, ground surfaces, and structural surfaces, the model implements additional mathematical relationships utilizing detailed vector analysis for thermal radiation blockings and ground reflections for general geometry. This is described in more detail below.

**Table 1**
**Material Property of Surfaces**

| | Thickness mm | Emissivity | Conductivity W/m K | Density $kg/m^3$ | Specific heat J/kg K | Tdamage Temp (K) | Tignite Temp (K) |
|---|---|---|---|---|---|---|---|
| Roof type | | | | | | | |
| Cedar shake | 25 | 0.85 | 0.156 | 395 | 2300 | 473 | 629 |
| Asphalt shingle—class A | 6 | 0.91 | 0.324 | 1560 | 920 | 473 | 642 |
| Tile | 9 | 0.9 | 1.4 | 1900 | 880 | 573 | 2000 |
| Exterior surfaces | | | | | | | |
| Vinyl siding + XPS foam | 0.93 | 0.89 | 0.145 | 1889 | 882.3 | 473 | 700 |
| Clear grade redwood T&G | 19.2 | 0.82 | 0.171 | 410 | 2512.5 | 473 | 600 |
| #2 ponderosa pine T&G | 18.5 | 0.83 | 0.169 | 420 | 2313 | 473 | 621 |
| Painted plywood | 12.8 | 0.83 | 0.211 | 500 | 2654 | 473 | 629 |

# 3. Determination of Radiant Heat Transfer

## *3.1. Tree Heat Release Model*

CalcTreeHRR is used during initial processing in the FireModel subroutine to calculate the heat release rate and burn time of the trees, given the tree foliar mass and leaf moisture content (MC). These values are used in the radiant heat transfer calculations and stored for file output. The model assumes the effective heat of combustion is 13,100 kJ/kg [16] for dried foliage and calculates the total heat release (THR) in kJ from a burning tree as the effective heat of combustion times the foliar dry mass, m (kg). There are two formulas for finding the peak heat release rate (HRR) one for Douglas fir and the other for all other trees. This lumping for the tree HRR reflects the current state of knowledge regarding tree HRR in kW as documented in the 4$^{th}$ edition of the SFPE Handbook in a chapter by Babrauskas [16]. For Douglas fir the formula is Equation 1 (from SFPE Fig. 3.1.67), and for all other trees the formula is Equation 2 (from SFPE Fig. 3.1.70).

$$HRR = \frac{2 \times m \times 400}{(1 + 0.0538 \times MC)} \tag{1}$$

$$HRR = \frac{2 \times m \times 700}{(1 + 0.1295 \times MC)} \tag{2}$$

Obviously there are tree species that are more fire resistance than the trees considered, but it does not matter if conservative evaluation is the goal. That is, the choice of relatively high flammable Douglas fir as a proxy for the less flammable species, only makes the model more conservative in its estimates of home ignitability, perhaps compensating for ignoring flame tilt or mulch on the property, or some other secondary features. However it would be beneficial to obtain HRR data of additional tree species for fire model refinement and further validation. In Equations 1 and 2 the mass is the foliar mass with water, which is calculated based on the given dry mass and foliage moisture content. Finally the total burn time in seconds is estimated as the total heat release (THR) divided by HRR, assuming a rectangular shaped HRR profile. With radiant power assumed as a constant fraction of HRR, the resulting surface radiant flux is constant during the tree burns, thus also allowing a simplified prediction of the rising surface temperature as occurring over a burn time.

## *3.2. Basic Radiation Heat Transfer Model*

The main radiant flux work is handled in CoreFlux subroutine, which breaks a surface into elements by calling a subroutine, and then calculates the flux from each tree to a particular element, using the CalcTreeQ function. Before calculating the radiant heat transfer, a subroutine called by CoreFlux checks to see if that element might be blocked by other trees or surfaces and returns the fraction of the tree fire radiation that reaches the element after being blocked or attenuated and

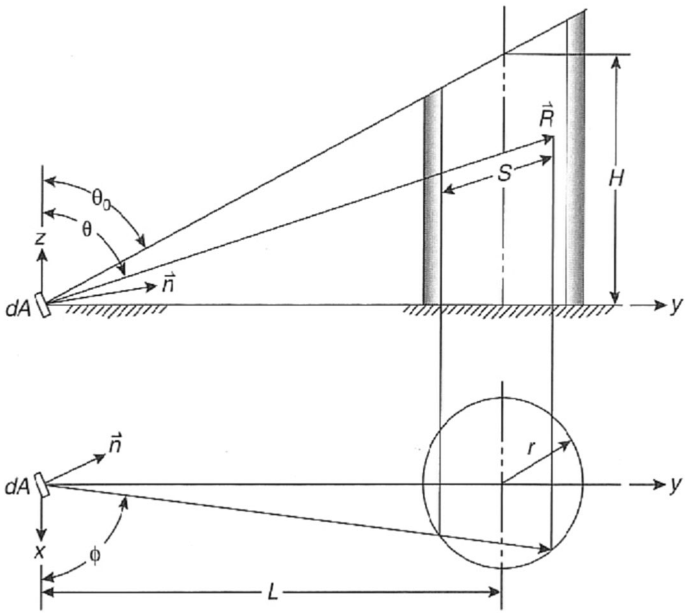


**Figure 1. Geometry for cylinder flame.**

is discussed later below. The radiant heat transfer calculation assumes the flame of the burning leaves is a cylinder, the flame is homogeneous, and its radiant properties are those of smoke similar to that of burning wood. Under these conditions the heat transfer from the source j is given by Equation 3 as outlined in the SFPE Handbook as Equation 47 in a chapter by Tien et al. [17].

$$q_j = \varepsilon_m E_b (F_1 + F_2 + F_3) \tag{3}$$

The F factors depend on the geometry for which the flame height is required. The geometry is pictured in Figure 1 (from SFPE Fig. 1-4.10) and defines the variables with which geometry F factors are calculated.

Given this geometry and assuming that $u$, $v$, $w$ are the x, y, z components of the unit normal vector n, normal to the surface, the formulas for geometry F factors are in Equations 4, 5, and 6.

$$F_1 = \frac{u}{4\pi}(rL)^2[\pi - 2\theta_0 + \sin(2\theta_0)] \tag{4}$$

$$F_2 = \frac{v}{2\pi}\left(\frac{r}{L}\right)[\pi - 2\theta_0 + \sin(2\theta_0)] \tag{5}$$

$$F_3 = \frac{w}{\pi}\left(\frac{r}{L}\right)\cos^2(\theta_0) \tag{6}$$

The vertical orientation angle of the element unit normal vector ($u$, $v$, $w$) s given by Equation 7.

$$\theta_0 = \arctan(L/H) \tag{7}$$

The horizontal distance to the center of fire is $L$, flame height is $H$, and flame radius is $r$. Since the view blockages were not considered in the formulation of these equations for extreme normal vector orientations, the view factor functions are interpolated to approach zero at extreme angles and distances to maintain the code robustness and continuity. Likewise, due to the formulation limitations, the view factor functions are adjusted to higher values for when the horizontal distance to the center of fire is less than the flame radius as described in Dayan and Tien [18]. The flame height was originally calculated from the heat release rate (HRR) and flame diameter (D) using Equation 8 as outlined in the SFPE Handbook as Equation 8 in the chapter by Heskestad [19].

$$H = -1.02 \times D + 0.235 \times HRR^{0.4} \tag{8}$$

However to prevent the flame height from going negative at low enough HRR, Equation 8 was supplemented by a new formula proportional to HRR and inversely proportional to D raised to the 3/2 power as described by Quintierre and Grove [20]. In evaluating the flame emissivity in Equation 3 the absorption coefficient $\kappa$ for smoke for wood was initially adopted as 0.8 $m^{-1}$ (from SFPE handbook value for wood) and the path length $S_j$ (in meters) is evaluated as the so-called mean beam length,3.6 $V_f/A_f$, which reduces to 90% of the crown diameter for tall flames, for use in Equation 9.

$$\varepsilon_{m,j} = 1 - \tau_j = (1 - e^{-\kappa S_j}) \tag{9}$$

The blackbody total emissive flux $E_b$ uses the Stefan-Boltzmann constant ($\sigma = 5.6696 \times 10^{-8} Wm^{-2}K^{-4}$) and the temperature of the smoke was initially adopted as 1732 K for wood. Thus $E_b$ had an initial value of 507.9 $kW/m^2$ from Equation 10. Both $\kappa$ and $T_f$ were adjusted as described below to give a much improved prediction of radiant flux.

$$E_b = \sigma \times T_f^4 \tag{10}$$

*3.2.1. Modification of Handbook Values to Improve Radiant Heat Transfer Calculations* As an internal test of the radiant flux formulation, the radiant fraction was calculated as the radiant heat from the cylindrical shaped fire and divided by the heat release rate, HRR, from Equation 11.

$$\chi_r = \varepsilon_m E_b A_f / HRR \tag{11}$$

Using this definition of the radiant fraction, and calculating radiant flux given different values of the flame diameter and the heat release rate, the radiant fraction was calculated as being typically above unity for the initial extinction absorption coefficient of 0.8 $m^{-1}$ and flame temperature of 1732 K. To account for the possibility of inaccurate assumptions about the cylindrical flame area (i.e. the actual flame necks inward to a somewhat smaller diameter flame than that of the base), a virtual cubical box was constructed around the virtual flame in the PC version of the fire model. The six internal surfaces of the box were broken into numerous small surface elements so that the heat flux for each element (via Equation 3) multiplied by the element area is the radiant energy to that element, and when added together for all the elements within the box provides the total radiant energy output for comparison to the heat release rate. The radiant fraction thus calculated was also typically above unity, and in agreement with Equation 11 values for the radiant fraction to within several percent. This result is inherently inconsistent with Tewarson's [21] measured data of radiant fraction for pine wood as 30% (Table 3-4.11 in 2008 SFPE Handbook). This motivated the thermal radiative flux measurements for this study.

To refine the heat flux calculation and verify the 30% radiant fraction, the radiant flux was directly measured with Schmidt-Boelter (SB) heat flux sensors on a vertical wall exposed to dead fuel litter burn in a wire basket. The HRR profile was measured as a function of time and used as an input to the Fire Dynamic Simulator (FDS) for the fire under the instrumented hood. The values from the SB heat flux sensors confirmed the setting of the radiant fraction at 30% in the FDS to get agreement with the heat flux sensor values, at least during the rise portion of the HRR curve (discussed more in the results). Fundamental work at Factory Mutual reported by Tewarson [22] for smoke production and radiant fraction also indicated a 30% radiant fraction for wood based materials and large pool diameters, and that fraction remains constant even after the smoke point has been surpassed at the higher HRR of a turbulent flame as described by Chatterjee, et al. [23]. Thus the constancy of the radiant fraction will have implications for the proper values for the flame radiation temperature, or the extinction coefficient, or both, that may change as function of HRR and fire dimensions.

Because the intent was to follow the flame geometry as shown in Figure 1, rather than more realistic necking in the flame that is simulated with FDS as demonstrated by Wen et al. [24] and other CFD models, an empirically based formulation was required for the flame radiant temperature and extinction coefficient that achieves the constant radiant fraction of 30% for a wide range of HRR and fire diameters. It has been well established that the extinction coefficient is proportional to the soot volume fraction and the flame radiation temperature. However, they will need to be reinterpreted from localized values to a global property value that assumes uniform temperature and extinction coefficient for the whole cylindrical volume. The paper of Dupuy, et al. [25] shows such an experiment with localized extinction coefficient and temperature measurements within the flame from a cylindrical forest fuel burner. As suggested in the paper itself, the measured extinction coefficient should be halved to adjust from the actual flame diameter to the larger diameter of the flame as modeled in Figure 1.

The flame radiation temperature is known experimentally to be relatively constant over a practical range of HRR, at least as reported by Dupuy, et al. [25] for forest fuel and Adiga, et al. [26] for propane fuel. The empirical formulation relies on the square root of the Froude number to calculate both the flame temperature and the extinction coefficient. The Froude number is a dimensionless number often used in fluid mechanics to describe the buoyant flow above a driving force, such as combustion. The geometry of turbulent diffusion flames scales with the two-fifths power of the Froude number according to Quintiere and Grove [20] and Dupuy et al. [27], calculated here in Equation 12 as in the form given in SFPE handbook in the chapter by Heskestad [19].

$$Fr = (HRR/D^{2.5})/1110 \tag{12}$$

This relative constancy of flame temperature with HRR was achievable (Equation 13), by prescribing the soot volume fraction to be proportional to the square root of the Froude number, thus making the "global" extinction coefficient proportional to square root of the Froude number and directly proportional to the temperature in Equation 14.

$$\begin{aligned} T_f = 1991 - 23.4(D - 0.019)^{0.044}(7.9 - D)^{1.73} \\ -425.4D^{0.457}/(1 + 0.166Fr^{1.069}) \end{aligned} \tag{13}$$

$$\kappa = 2.8 * (T_f/1353) * (Fr/3.96)^{0.5} \tag{14}$$

Equations 13 and 14 also provided relatively good agreements of both flame temperature and extinction coefficient (by doubling it to adjust for flame necking) with data of Dupuy et al. [25]. For practical values of $Fr$ between 0.2 and 10 the error in predicting the radiant fraction of 0.3 with Equation 11 is at most 7%, and is within 1% for the litter burn tests with values of $Fr$ between 0.15 to 0.77 (or 35 kW $<$ HRR $<$ 250 kW for 0.61 m fire diameter). Note that Equation 13 is valid for fire diameters between 0.019 m to 7.9 m which covers nearly all known experimental data for vegetation fires. In the interest of keeping robust calculations with the ecoSmart Fire model, the flame radiant temperature formula utilizes an adjusted fire diameter that is limited to be within 0.019 m and 7.9 m. Thus it is found that the extreme values of the flame diameter (less than 0.019 m or greater than 7.9 m) will result in the radiant fraction being greater than 0.3 but less than 1, for which no experimental data exists in any case. The flame emissivity computed (with Equation 9) shows a good correspondence with the data presented by Agueda et al. [28] for their measurements with combustion of forest fuels. Fuller details on the derivation of Equations 13 and 14 and other aspects of thermal radiation modeling will be provided in another publication, as the focus of this paper is a laboratory verified physics-based model to calculate home ignitability from the thermal radiation threat, and thus better define defensible space for any given set of ornamental vegetation and structure cladding as required in NFPA 1144.

*3.2.2. Final Refinements to Flux Calculations* The CalcTreeQ function performs these core radiation calculations (Equations 3 to 14) while also ensuring that the surface element has a direct line of sight to all four corners of the burning tree crown. A few accommodations for the geometry are required to allow CalcTreeQ to function properly. These adjustments are handled in the CoreFlux function as the contribution of each tree is added to the total for the surface. The main outer loop works over each surface element, ise, and the coordinate system is reset so that it centers on the element. Then for each tree a baseT, the bottom of the flame, and a topT, the top of the flame, are defined based on the bole height, flame height, and vector to the tree. Finally the total flux is calculated as the sum or difference of two CalcTreeQ results depending on the location of the flame relative to the z axis. This calculation is necessary since the core geometry assumes the flame starts at height zero and goes up. But in fact the flame base could be above or below the surface element. If it is above, then the total flux calculated by the top of the flame needs to be adjusted to subtract out the flux from flame that does not exist from height zero to the bottom of the flame. Similarly, if the flame is both above and below the zero line, then the two components which calculate from the zero line are added together to get the total flux.

### 3.3. Methods for Calculating Object Blocking, Ground Reflection and Tree Flame Attenuation

The irradiance from the tree fire source j as given in Equation 3 is reduced by any blocking building surface k apart from that corresponding to the surface element ise, by ground reflectance $R_{j,}$ and by any attenuation through a blocking burning tree, k. Additional refinements are added to CoreFlux to handle the ground reflection of thermal radiation from each tree fire to the surface element. These refinements depend on the FireModel making a duplicate of each. Then in CoreFlux the calculations for these duplicate trees process it as the reflected images of the actual tree fires across the ground plane. Specifically the baseT and topT which define the flame region are mirrored over the z axis so the flame appears underground, and thus the line of sight to the structure surface element is different. Similarly when the flux is calculated only the reflected thermal radiation fraction, using the local ground cover reflectance, is added to the total heat input for calculating the temperature rise for that surface element.

Vector algebra is used to efficiently determine the blocking by a building surface. That is, the projected polygon area of the tree fire cylinder as viewed from the heated surface element is computed in the plane of the building surface, which then is used to determine the area overlapping with the building surface area for blocking fraction determination. This efficient computation is an approximation to the more accurate approach of dividing all objects into surface elements and connecting all such surface elements with lines, and that blocking occurs when such lines intersect surface elements in between the targeted surface elements. For the overlapping area approach, the four vectors from the surface element ise to the four corners of the edges of the cylindrical tree fire j are entered into the subroutine containing the object blocking algorithms. Each structure surface has a planar equation defined by a line vector emanating from any point in the plane and dotted with the surface normal vector, with the dot product set equal to zero. The intersections of the plane with the four vectors from the element to the four corners of the tree fire cylinder j are calculated and four projection vectors from the surface element ise to the plane then terminate at the intersection points of a polygon area. However, it is possible that one or more intersection points fail to be calculated (i.e. Divide check) and the structure surface is then not blocking, and its viewing fraction is unity. In any case, all four projection vectors must have lengths shorter than the corresponding flame viewing vectors from the element ise, to qualify as a candidate for blocking the view to the tree fire j. The projection vectors end-points form a projection quadrilateral which is then compared to the candidate surface quadrilateral to determine any overlapping area $A_{ov,\ k}$ via an intricate logic process and vector analysis algorithms. The overlapping area is subtracted from the projected quadrilateral area $A_{proj,,k}$ to determine the non-overlapping projected area, which is then divided by the projected quadrilateral area, to determine the viewing fraction. This is shown in Equation 15 below in which the irradiance from the tree fire j is being reduced. Note that the attenuation transmittance of a structure surface is zero and the ground reflectance is unity for a direct line of sight from the tree fire j. Of course, if a viewing fraction is zero, then no further blocking or viewing calculations with other structure surface or attenuation by a blocking tree fire is needed and so then it exits early from the subroutine. However, for multiple blockings/attenuations, the viewing fractions are multiplied together for best consistency and approximation to the actual geometric viewings associated with multiple blockings.

$$q_{j,ise} = q_j R_j \prod_{k=1,n}^{k \neq j} \left[ (A_{proj,k} - A_{ov,k})/A_{proj,k} + \tau_k (A_{ov,k}/A_{proj,k}) \right] \tag{15}$$

If all the view fractions determined by the structure blocking algorithms are non-zeroes, then the tree fire attenuation subroutine determines any tree blockings. Since the four cornering viewing vectors to the other tree fires k from the element ise already exist, they are used to define a quadrilateral of tree fire k for a potential blocking of the tree fire j. This quadrilateral is compared with the tree fire j projected quadrilateral on the same plane to determine the overlapping area as done in the similar algorithms as before. Of course, all four projection vectors must be less than the corresponding four flame viewing vectors to be a candidate for attenuation blocking and therefore is used in Equation 15. The formula for transmittance though the blocking tree fire k is in Equation 9 for the flame emissivity. A fuller description of radiation blocking that includes formulae and algorithms is reserved for a later publication.

### *3.4. Determination of Damage and Ignition from Material Properties*

Since damage and ignition are based on their critical surface temperature values, a transient heat conduction model is used to calculate the cladding surface temperatures at the element ise in response to numerous radiant heat loadings and convectively cooled by ambient winds. For all combustible materials in Table 1 the damage temperature is approximately 200 Celsius (473 K) as the wood begins to darken, or the vinyl begins melting, or the asphalt shingles loses integrity. The roof tile is a non-combustible material that when heated enough can cause damage to the underlying plywood, and thus a damage temperature of 300 Celsius (573 K) is used conservatively to indicate the hidden plywood charring. The various piloted ignition surface temperatures of combustible claddings are based on the transient heat conduction modeling from cone calorimeter tests [29]. The accurate empirical formula for finitely thick materials as exposed to radiant heat flux kept constant with time and cooled convectively was presented in the form of irradiance as a function of time to spark ignition of several tests on the material. Since material density, surface emissivity, and convective heat transfer coefficient were determined prior to the tests, the reasonable values for ignition temperature, heat capacitance and thermal conductivity of the material were derived from the least squares fitting of the empirical formula to irradiance versus time to ignition data. For utilization in the EcoSmart Fire model, the empirical heat conduction formula was analytically inverted to provide surface temperature as functions of fixed irradiance and heating time while using the measured or derived properties of thickness, emissivity, conductivity, density, and specific heat. The prediction formula for the surface temperature rise from an imposed heat flux q is from Dietenberger and Grexa [29],

$$T_s(t) = T_a + (\varepsilon_{ise} q/h_{ig}) \Big/ \left\{ 1 + (F_{thick}^n + F_{thin}^n)^{(-1/n)} \right\} \tag{16}$$

where,

$$\varepsilon_{ise}\, q_{cr} = h_c(T_{ig} - T_a) + \varepsilon_{ise}\sigma(T_{ig}^4 - T_a^4) \equiv h_{ig}(T_{ig} - T_a) \tag{17}$$

$$n = (2.68 + 0.4Bi)/(1 + Bi) \tag{18}$$

$$F_{thick} = \sqrt{\frac{4}{\pi} Bi^2 Fo} \tag{19}$$

$$F_{thin} = \exp\left(\frac{BiFo}{1 + 0.254Bi}\right) - 1 \tag{20}$$

$$Bi = h_{ig}\delta_m/k \tag{21}$$

$$Fo = (k/\rho c)t/\delta_m^2 \tag{22}$$

Under fixed irradiance and when the heating time t in the Fourier number, Equation 22, increases to the ignition time, the predicted surface temperature becomes the ignition temperature. Note that if the ignition time is infinite, and with the surface temperature at the ignition temperature and the imposed heat flux at the critical value, then Equation 16 reduces to Equation 17, which describes that the convective and radiative heat losses that just compensates for the imposed irradiance (and thus no more heat flows into the material). The effect of the material thickness is contained in the Biot and Fourier numbers. So, if the heating time is greater than the ignition time, the predicted temperature will be greater than the ignition temperature, and so signifies a piloted ignition condition.

The properties determined are provided in Table 1 for thickness (mm), emissivity, conductivity (W/m K), density (kg/m$^3$), specific heat (J/kg K), damage temperature (K), and ignition temperature (K). Values of conductivity and specific heat correspond to the temperature at halfway between ambient and ignition and low moisture content as given in Dietenberger and Grexa [29] (roof tile uses generic value for concrete). For these same materials the effect of temperature and moisture content on the thermal properties were obtained, but in which the worst case weather of dried conditions was assumed here. A table of choices with associated properties is maintained on the web server, so the end user picks a roof or surface type from a drop-down list, and the related properties are passed to the fire model. Table 1 provides the labels and a sample of the values provided for select roof types and exterior cladding surfaces.

It is noted that in the worst case scenario it is expected that the firebrands will be the main source of a pilot and not necessarily the irradiance source like the burning trees are. However, the trees will have a finite burn time and as several trees are burning, there will be multiple irradiance sources to the surface element. For an efficient web based application all start times are set to zero. Then trees with the same moisture content have similarly calculated burn times, such that the maximum surface temperature reached is a special case as,

$$T_{s,ise,\max} = T_a + \sum_{j=1,n} q_{j,ise}[T_s(t_{bj}) - T_a]/q \tag{23}$$

After the calculation of surface temperature of each element, the subroutine, CalcDamage, compares the surface temperature prediction with the damage temperature. In the output summary for the structure surface, the subroutine determines the number of elements with surface temperature exceeding the damage temperature threshold as divided by the total number of elements in the surface. Likewise, the fraction of elements whose predicted surface temperature exceeds the ignition temperature for the selected building surface is also entered into the text file. The same sort of calculations are done for each structure surface and entered into the text file. For PC applications additional outputs of the heat flux distribution on the surfaces, and also of surface temperature distribution can be provided for contour plots.

In the current implementation of the fire model the heat release is determined for Douglas fir separately from all other tree species because extensive data for Douglas fir are available. The entry for Foliar Mass is the dry mass of the foliage, given in kg. The Moisture Content is an indication of the percentage moisture in the foliage. To simplify end user input the system defaults 20, the value of dry foliage. Other possible values that could be used in a different implementation can be selected. The local ground cover reflectance is a number between 0 and 1 that specifies what percentage of incident heat is reflected off the ground near the tree to the structure. Again to simplify end user input the system defaults 0.3 for the reflectance, but other reasonable values can be selected.

## 4. Validation of Radiant Heat Fluxes

Various formulae go into the determination of the irradiance on any particular surface element from a cylindrical shaped fire in the model, and must be validated with fire tests. Some formulae were well established, such as the view factors and the flame height, while the formulae for flame radiant temperature and extinction coefficient needed to be derived empirically to ensure the radiant fraction is constant at 0.3, as calculated via Equation 11. This was the basis for the dependency of extinction coefficient and flame radiation temperature on the HRR and D. Because the flame height is a function also of HRR and D, the radiant heat flux on any surface element can be calculated with Equation 3 with only just knowing HRR and D of a fire with a prescribed radiant heat fraction. Experimental data have shown that the fires of the following fuels, pine wood, dead litter and propane, have the appropriate radiant heat fraction of 0.3. The dead litter fuel was already mentioned as used in validation of Equations 12 and 13 and will be discussed in the following, but has a HRR that changes with time, with a ramping of HRR to a peak, and then an exponential-like decay (FDS snapshot result at peak HRR in Figure 2). A constant HRR source will be needed to validate the surface temperature prediction in response to a constant irradiance, for which a floor-level propane burner was used to provide heat to vertical redwood boards with surface thermocouples attached. The use of propane was appropriate with a radiant heat fraction of 0.3, as also verified by the FDS simulation of the 12 inch square pilot burner as heating the SB heat flux sensors on the mockup vertical wall (red back wall shown in Figure 2) adjacent to the burner (propane burner not shown in Figure 2).

### *4.1. Surface Irradiance Validation with Litter Fire*

For proper testing, the fire diameter D and the pool-like heat release rate HRR as a function of time must be measured, while the two SB heat flux sensors (at heights 1.21 and 1.56 m) inserted in the mockup back wall measure the irradiances as a function of time. For burning the litter fire completely, a chicken wire round basket was constructed that fitted on a 0.61 m diameter pan and also setting on a thin absorbent paper soaked with the methanol accelerant. This test

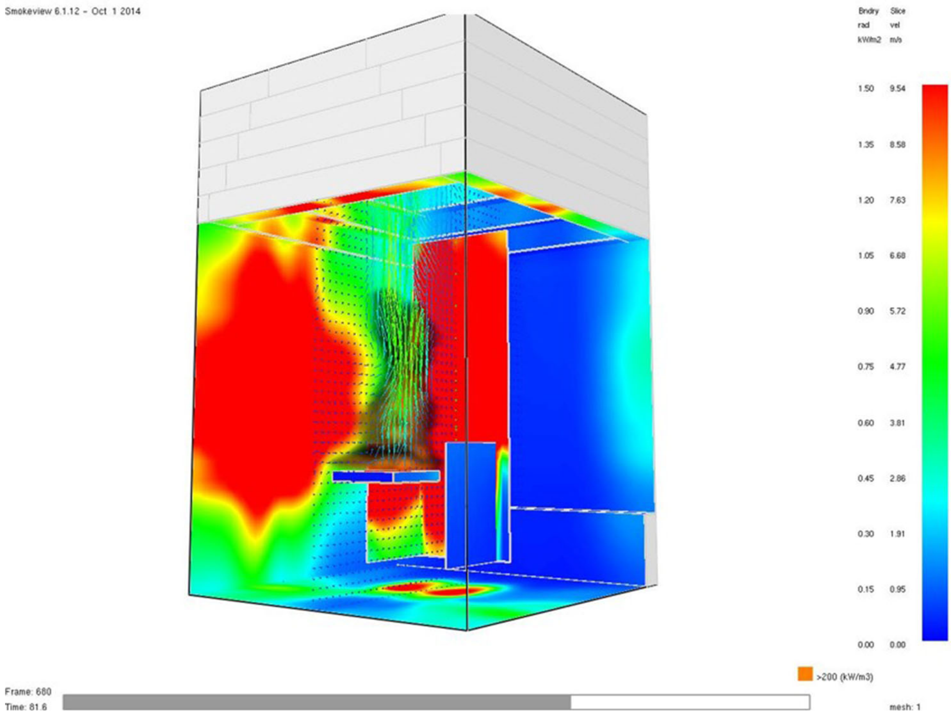


**Figure 2. Litter Burn over a circular bed aside a mockup with SB heat flux sensors in the mockup vertical wall under HRR Hood and FDS results—Radiant Fraction Equals 0.3 for agreement with SB heat flux sensors values.**

holder was also set on a weigh scale to monitor mass loss as a function of time. Ignition of the methanol accelerant insured an intense and complete burn of the typically 4 inch thick litter layer. The HRR was measured as a function of time with the test under the instrumented hood using the procedure described by Dietenberger and Boardman [30] for measurements with smaller fires (Figure 3). This provided data to determine the global properties of flame height, extinction coefficient and flame radiation temperature, sufficient to determine irradiances with Equation 3 and shown in Figure 4. Good agreement of the modeled heat fluxes with measured heat fluxes occurring during the rise portion of the HRR was expected. However, the under prediction of the heat fluxes during the peak and declining HRR is likely the result of not accounting for radiance from the heated pan and mockup side arms (blue side panel in Figure 2) during the heating phase in the current ecoSmart fire model. The modeling with FDS showed a similar agreement of the heat fluxes during the rise portion of the HRR. The setup for FDS model included the heated pan and mockup side arms, but provided an over prediction of the surface heat fluxes during the decreasing portion of the HRR, probably due to not attributing the measured HRR to glowing combustion on the

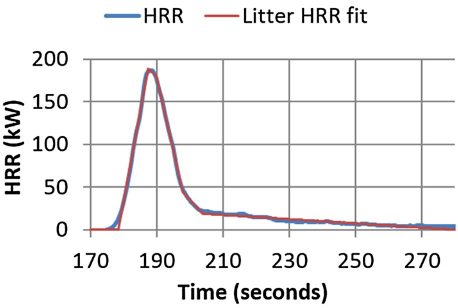


**Figure 3. Piecewise function fit to the litter HRR profile for input to FDS and ecoSmart Fire PC model.**

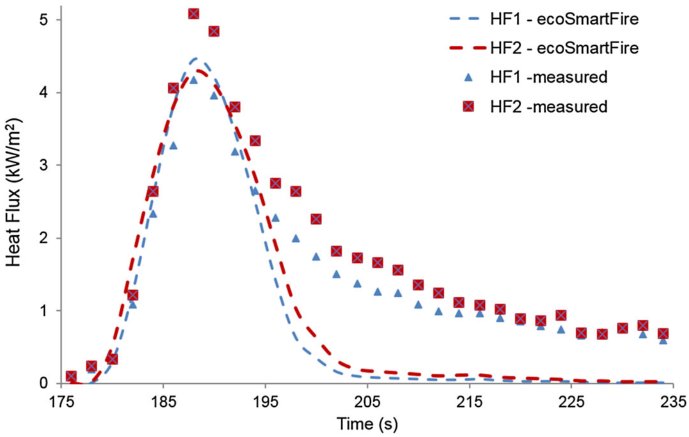


**Figure 4. Prediction of high and low orientated radiant flux values on mockup vertical wall due to litter fire.**

pan rather than to the nearby flaming combustion as in the current model. These hypotheses can be further improved by obtaining additional experimental data and comparing to modeling results. The heat flux sensors themselves have at most a 10% error.

### *4.2. Surface Irradiance Validation with Propane Fire*

The propane burner was placed on the floor near the mockup, rather than on the mockup platform, because it was desired to also heat vertically mounted redwood boards set on the floor. This resulted in heat fluxes on the mockup that were lower and at different angles than that of the litter burn. The effective diameter of the fire was computed as 0.335 m that has the same area as the 12 inch (0.3 m) square burner. The HRR was measured as a function of time with the test under the instrumented hood in which three levels of HRR were programmed (Figure 5). The fitted HRR function was input to the fire model to provide the calculated

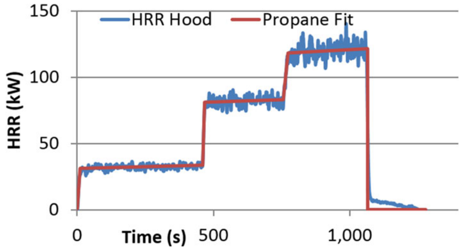


**Figure 5. Piecewise function fit to the propane HRR profile for input to FDS and ecoSmart Fire PC model.**

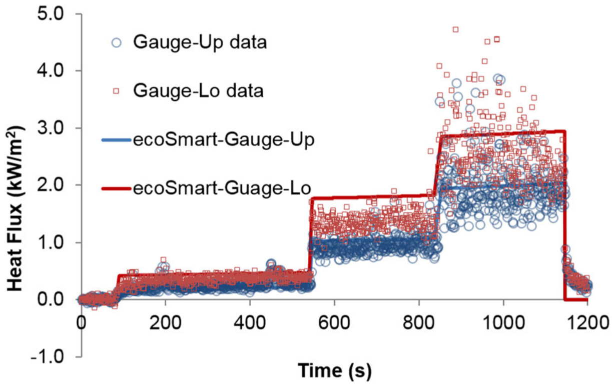


**Figure 6. Prediction of high and low vertically orientated radiant flux values on mockup due to propane fire.**

radiant fluxes in agreement with the noisy SB heat flux sensor values (Figure 6). The use of the 0.3 radiant fractions continues to be confirmed, this time for the propane burner.

## *4.3. Validation of Temperature Predictions with PC Implementation*

Vertical redwood boards were set near the propane burner with five surface thermocouples, one in the center, and four near the corners (Figure 7). The positions of the thermocouples were measured relative to the burner center, which upon inputting, along with D and HRR, into the fire models, resulted in heat fluxes to the five positions from the evaluations of Equation 3. The thermal properties for the redwood are listed in Table 1 for use in the evaluation of the surface temperature calculated with Equation 23. Only the data for thermocouples #4 and #5 are presented in Figure 8 to reduce cluttering of the graph, and to show fair equivalence between the FDS and ecoSmart Fire model predictions of the surface temperature response to within about 10 to 20% error (dependent to a nearly square

**Figure 7. Vertically mounted redwood boarding with edges showing the pitch oozing out from radiant heating by the propane pool fire.**

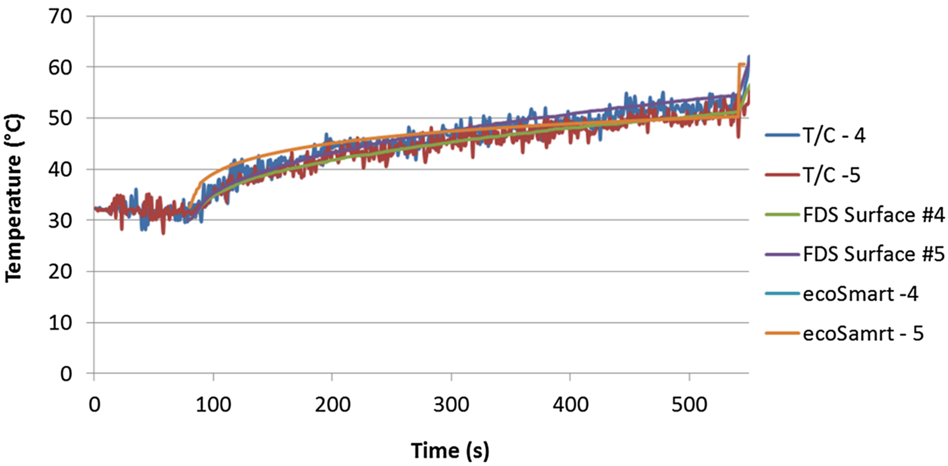


**Figure 8. FDS and ecoSmart Fire predictions of surface temperature at locations #4 and #5.**

root of time) to relatively constant heat fluxes. Obviously, there are many other potential positions for the redwood boards, many other HRR profiles (including those high enough to achieve piloted ignition), and other materials that can be tested for further model validations and error estimations. The error in the thermocouple readings is typically less than 3 K.

## 5. Example of ecoSmart Fire Model Predictions Using Website Implementation

The optimum positions and sizes of ornamental trees and shrubs on a property are dependent not only on their fire risk, but also on the affected water table, energy usage, and carbon balance [15]. This led to landscaping choices directed towards being implemented on a website that uses homeowners input on a convenient geographical platform, known as ecoSmart Landscapes (Figure 9). This also leads to certain compromises on the model features in coordination with the other modeling teams involved in calculating carbon balance, energy usage, and water table as well as the limited computing abilities of a website implementation. The website version is limited to 4 walls and 1 flat roof, choice of redwood or vinyl wall, choice of asphalt shingle or cedar shakes roofing, and up to 9 trees total anywhere on the property, all to save on computation time in sharing of core models for carbon balance, energy usage, water table, and fire risk. One benefit of this platform integration is that the tree species, dimensions and weight are an output from the shared core models which are then used as an input to the fire model, meaning that the homeowner can have access to the tree growth modeling up to maturity for their fire hazard analysis. To simplify the input conditions, the trees for the worst case scenario are dried at 20% MC, the wind speed set at

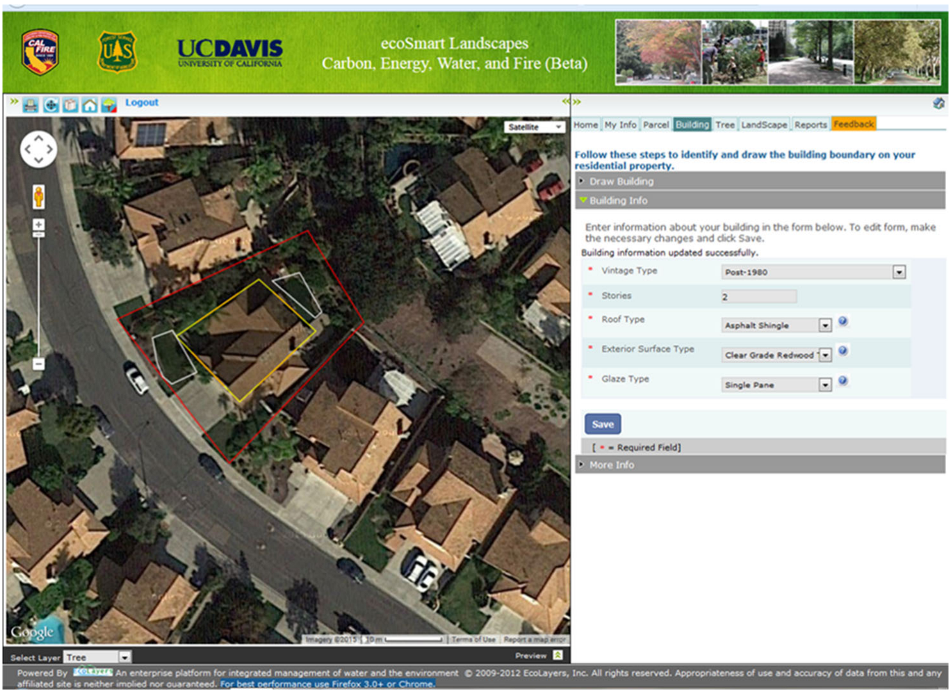


**Figure 9. Setting up input to Fire Model within the ecoSmart Landscape web-based application that uses Google Earth input.**


**Figure 10. Selection of 3 trees along first wall (NW) (3 green dots near yellow line) and 1 tree at the corner of third and fourth walls (SE) (green dot near driveway) (Color figure online).**

5.7 m/s, and the ambient temperature is 25 degrees Celsius. Obviously the architect or landscape engineer may prefer the PC version that is not limited by these website feature choices. In Figure 9 the Beta version ecoSmart Landscapes was used to locate a property in California and for which the parcel outlines (red), building drawing (yellow), and vegetation for water usage (white) are initially drawn. Next, as shown in Figure 10, 3 trees are selected on the NW side of the parcel across from Wall #1, and 1 tree is selected on the SE side of the parcel across from Walls #3 and #4, to do the fire modeling.

### *5.1. Model Results—Heat Flux Distribution Example on Building Surface*

Wall #1 (NW side) with the highest heat flux exposure was chosen among the heat fluxes predicted for the 4 walls and the flat roof top for presentation in Figure 11, which is a contour plot of the flux at each surface element evaluated. Horizontal and vertical units indicate the element number with each element near 0.35 m square in size. The 3 large trees were purposely chosen to produce the heat

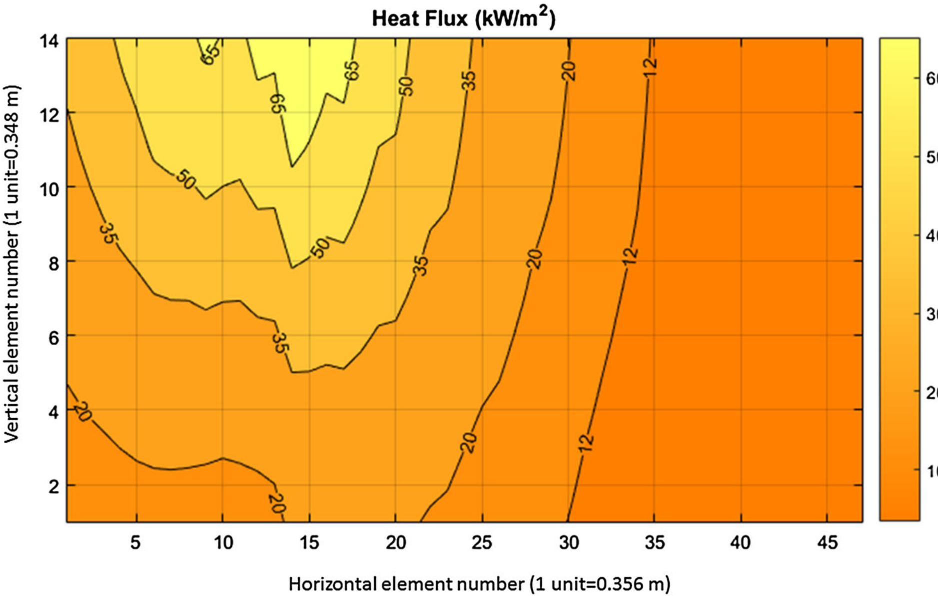


**Figure 11. Predicted heat flux (kW/m$^2$) on Wall #1 from 3 burning trees on NW side.**

flux ranges on the wall that would normally be burning in the presence of a pilot if heated long enough. It is noted that at horizontal distances larger than 9 to 11 m (30 to 35 ft) to the right, the wall is considered safe from ignition because of the 12 kW/m$^2$ isoline for critical heat flux level typically used to define safe distances between buildings. However, the tree burn times are around 30 s, instead of the 30 min or greater for the building burn times which typically inform the safe heat flux criteria. Thus the actual region safe from ignition will be larger when based on not exceeding the surface temperature for piloted ignition. Calculating the surface temperature requires a transient heat transfer analysis such as is included in EcoSmartFire.

### *5.2. Model Results—Surface Temperature Distribution Example on Building Surface*

With Wall #1 (NW side) of redwood siding as the chosen example for ignition analysis Figure 12 shows a contour plot of the temperature at each surface element evaluated. Horizontal and vertical units indicate the element number with each element near 0.35 m square in size. Thus Figure 12 shows the maximum temperature rise distribution due to all the trees burning simultaneously. Since redwood has an ignition temperature of 327°C according to Table 1, Figure 12 shows that the walls below 1.2 m (4 ft) high and further than 7.6 m (25 ft) across to the right are safe from ignition. This is a significant difference over that of using a critical heat flux criteria discussed in the last section. That is, 30% of wall is

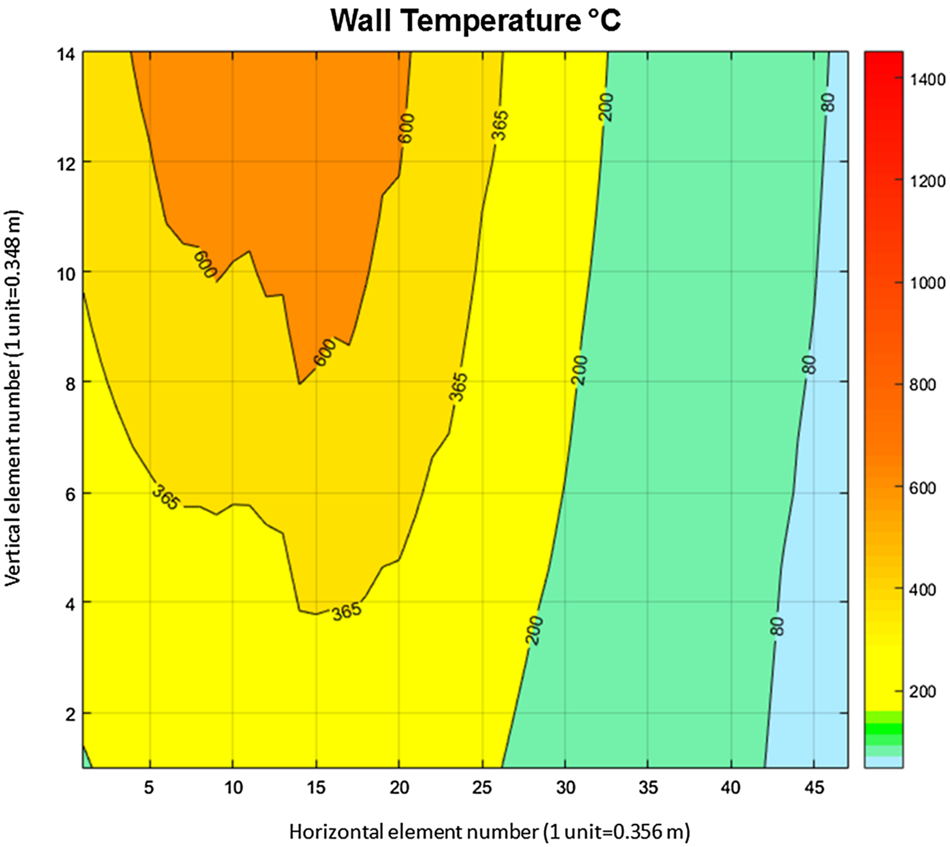


**Figure 12. Predicted surface temperature rise (Celsius) on Wall #1 (NW) with redwood siding for approximately 30 s burn time of heat flux exposure shown in Figure 11.**

ignited by temperature criterion as compared to 81% of wall ignited by the flux criterion. Indeed, with the model the thickness of redwood siding can be decreased to a theoretical paper thin level where 81% of the wall would ignite, thus agreeing with the flux criterion for surfaces ignited. Or in other words the actual thickness and heat capacity of the redwood siding limits the temperature rise given the short burn time, thus highlighting the usefulness of the transient heat transfer analysis built into EcoSmartFire. Finally, with the damaging temperature set at 200°C, the walls further than 9 m (30 ft) would be safe from discoloration damage, and thus is shown in green. The isoline for 80°C is shown to indicate the boundary for completely undamaged siding (blue region) to ensure no pitch oozing out for redwood (or in the case of vinyl siding, no distortion). The particular isoline temperature values will need further verification with specialized bench scale experiments. Figures 11 and 12 are not available for the website implementation due to the computation requirements of contour plotting.

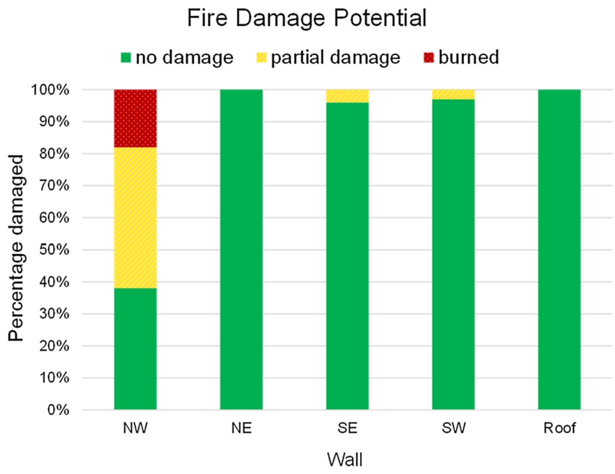


**Figure 13. Predicted fire damage potential for 4 redwood siding walls and 1 shingle roof (see Figure 10) for approximately 30 s burn time of heat flux exposures.**

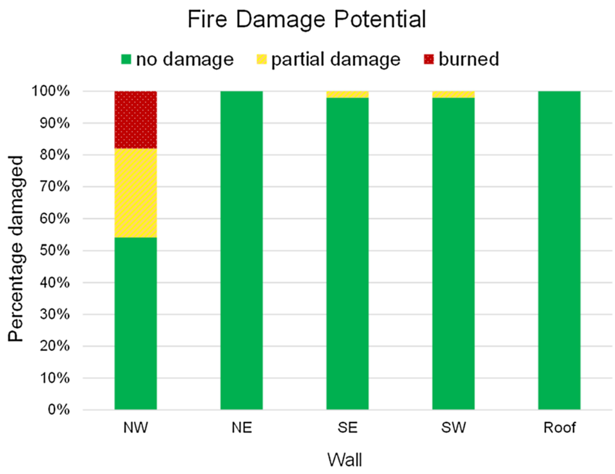


**Figure 14. Predicted fire damage potential for 4 vinyl siding walls and 1 shingle roof (see Figure 10) for approximately 30 s burn time of heat flux exposures.**

### *5.3. Model Results—Website Damage Summary on all Building Surfaces*

A more graphic approach is to summarize the damage on the five building surfaces (4 walls and 1 roof) with a simple bar graph. It would be enough for a homeowner to determine the fractions of building surface that is undamaged (green), damaged from discoloration (yellow), or burned (red), as shown in Figure 13 for redwood siding and Figure 14 for vinyl siding for the 5 building surfaces shown. This is a simple calculation in the core fire model that is provided in the output file, and readily plotted on the website as shown. The bar graph for NW (Wall #1) show prediction of about 20% of the wall burned, 40% of the wall damaged, and 40% of the wall no damage. The bar graphs for SE (Walls #3) and SW (#4) show small damage from the single tree burning on the SE side of the parcel. The homeowner will first focus on reducing fuel from the three trees along the NW wall. Options include removing one or more trees, or regular pruning to remove biomass. Upon closer examination of Figure 10, it is evident that the neighbor's house to the NW is actually closer to the three trees than the resident's, so the neighbor might be consulted. Options to discuss in addition to tree management include installing a fire-rated wall or a tall noncombustible fence, a multi-structure feature that is available in the PC version. Also, the parties may agree to accept the risk associated with allowing some damage from a fire, as long as none of the building surface areas reach a burn status. This approach may be an acceptable alternative to the requirement of a 61 m (200 ft) vegetation clearance, if reached through consensus and the use of scientifically sound software, such as ecoSmart Landscape.

### *5.4. Model Results—Surface Temperature Prediction Distribution for 30 min Burn Time*

To further illustrate the benefits of the temperature based criterion imagine ways in which the burn time could be extended from 30 s to 30 min. For example, imagine that dead trees or wood are being fed to the bonfires with the same locations and HRR as the earlier tree burns for 30 min, which is long enough for structure temperatures to reach steady state at an elevated level. Alternatively, a high treehouse or a tall wood crib can be constructed and burn for 30 min at the same locations and HRR as the earlier tree burns. The surface temperature prediction in such a scenario and with redwood siding is shown in Figure 15. Now note that the predicted temperature isoline that would correspond to the 327°C ignition temperatures is within a half of a meter or less of the 12 $kW/m^2$ critical flux isoline shown in Figure 11. This means that the prediction of surface temperature at ignition can replace the critical ignition flux at equilibrium as the primary criterion for fire safety. Continuity with the existing codes regulating the spacing between buildings can be achieved with this new fire performance design criteria. That is, if a wall fire of a burning building can be modeled to provide radiant fluxes and burn time on an adjacent building surface, the criteria of surface temperature at ignition would be an equivalent fire performance measure as that for the building spacing based on critical fluxes. Indeed, greater flexibility in the spacing between buildings can be achieved if the burn time of a cladding itself is shortened by design to be much less than 30 min so that the imposed heat fluxes much higher than critical on an adjoining building surface can be achieved without the occurrence of ignition.

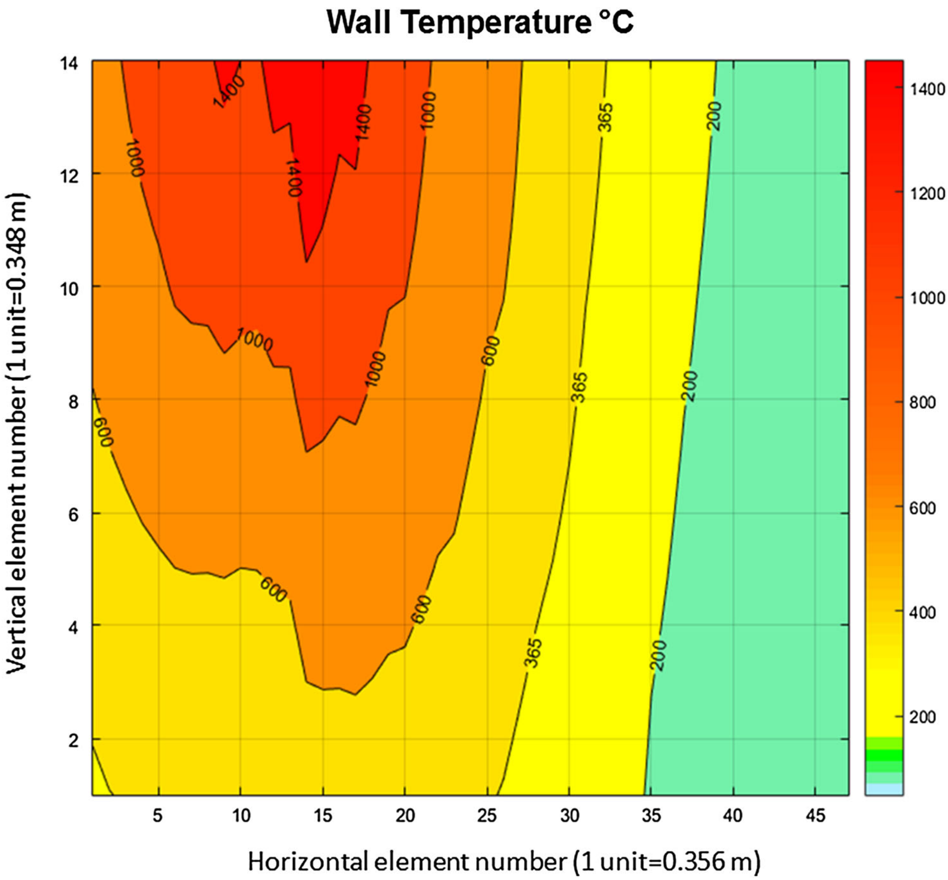


**Figure 15. Predicted surface temperature rise (Celsius) on Wall #1 (NW) for the 30 min burn time of heat flux exposure shown in Figure 11 for northwest side of house.**

## 6. Conclusion

Even though the EcoSmart Fire model advances the state of art in the quantitative assessment of home ignitability, the user needs to be aware of various limitations so that the model is most effectively used. There are various current limitations, such as physical process modeled, the amount of model validation, and the software environment. Regarding the physical processes, the physics that is being modeled is the damage and piloted ignition of structure surfaces as subjected to a worst case scenario of numerous small firebrands and irradiation from nearby peak burning of ornamental trees and shrubs. This is a conservative approach to defining the spacing between vegetation and building as the modeling of fire growth and spreading from one item to the next is presently impractical both from the state of art fire science modeling, and limitations due to it being a web-based implementation. Within the constraint of modeling on the PC, the ignitibility assessment was designed to accommodate multiple and any sized and complicated buildings as well as many ornamental trees and shrubs in varying atmospheric conditions of temperature, wind, and moisture content. This complicated geometry also led to the unique development of algorithms for efficient calculation of radiation blocking and attenuation as well as significant radiant reflections off of level ground. This complicated geometry also involved constructing many surface elements on structural surfaces that will be potentially damaged and ignited. The formulae for tree HRR, flame height, flame radiation, viewing factors, and transient surface temperature rise are quite well established on their own merits. New empirical modeling, however, was required of the global flame radiation temperature and the extinction coefficient, to provide a radiant heat fraction of 0.3 for vegetation fires, and yet provide reasonable values agreeing with laboratory tests associated with burning litter in a wire basket. They were modeled together for the first time here, and so their integration needed validation with testing under a heat release rate hood.

Regarding model validation, only limited results were presented with the litter fire in a wire basket and with propane fire from a floor burner. The radiant heat fluxes from these fires were measured with SB heat flux sensors in a vertical wall of a mockup, and shown to be in agreement with that predicted from the ecoSmart fire model as well as that from the FDS. Surface temperatures measured on a vertically orientated redwood boards were reasonably predicted by both the ecoSmart fire model and FDS to within about 20% accuracy, both using the same thermal properties for the redwood. Additional model validations for comparison with specialized fire tests, including those with flame tilt, are suggested for further refinements of the fire model and for estimating errors more carefully so that a factor of safety can be estimated.

Regarding the software environment, because of the current conservative aspects of the fire model to calculate the radiant flux threat and of its reliance on NFPA 1144 for hardening against firebrands and removal of adjacent ladder fuels such as litter, mulch, and woodpiles, it is practical to use as designed on the ecoSmart Landscape website despite lacking numerical values for factor of safety. The conservative aspects include (1) introducing damage temperature, which is usually much less than the ignition temperature, meaning avoidance of "yellow" bars in the fire assessment bars, (2) using the highly flammable species as a proxy for the lesser flammable vegetation, (3) choosing hot and dry conditions for the burning of vegetation, and (4) assuming all vegetation ignited simultaneously from a wildfire event. At least the model in its current version provides numerous options for vegetation landscaping and structure cladding as compared to the current situation with anecdotal knowledge that can be fraught with errors or misconceptions when dealing with effects of radiant fluxes from burning objects.

To have reasonable computer time and be consistent with other EcoSmart Landscape applications, the web-based application is limited to one flat roof (i.e. less than or equal to 3:12 slope), four vertical side walls, and nine trees anywhere on the lot. Although most homes have sloping roofs, which correspond to the use of wood shakes or shingles, the use of Class A roofs would make the website calculations for flat roofs as being more academic. The website user is limited to just a few representative building materials, which had been adequately tested at the Forest Products Laboratory (FPL) fire test laboratory for their material properties. An example of ecoSmart Landscape evaluation of a home site in California was shown, that seemed to provide reasonable results. Thus the website user can do damage and ignition modeling of various simple structures on the property, by doing them one at a time with the web-based application. For example, a singular rectangular decking with side walls can be investigated for exposure to nearby ornamental tree burning. Of course, ignitability assessment of all such structures using many more trees and shrubs with additional selections of cladding materials on realistic building with sloping roofs can be done simultaneously on the PC version, but more work is needed to replace the front end supplied by the web implementation. Even without that the core calculations are useful for researchers. For example, we recently examined the effect of up to five rows of six burning trees along a wall, with variations to the vegetation clearance distance, fencing, ground preparation, and cladding materials. Results were obtained that were not evident with anecdotal knowledge. For example, the calculations of representative scenarios have been allowing large trees to be within 1.5 m (5 ft) of a building surface whereas 3 m (10 ft) is typically required between buildings themselves that have fire resistance ratings and at least 9 m (30 ft) for unprotected walls (Table 602 in 2009 International Building Code Commentary). Indeed by inputting 1800 s burn time instead of the 30 s burn time, it is found the ignition temperature criteria provided equivalent result to the critical heat flux criteria for defining the regions of no ignitions on the walls. A new methodology that uses fire performance approach similar to that used for spacing between vegetation and building as described here should be utilized for the spacing between buildings also. As part of fire performance approach the flame tilt and litter deposits would be a consideration in modifying the spacing between the flammable objects. This would dispense with the complexities of tables that prescribe spacing between complex buildings.

## Acknowledgements

Initial inspiration to undertake this rewrite of EcoSmart Fire was provided by Greg McPherson and Joe Purohit who worked on the larger ecoSmart landscapes web project with funding from CalFire. Part of the core EcoSmart Fire programming work was supported under their CalFire contract. Greg and Joe helped shape the initial scope of the project. Further validation work and continuing software refinement was supported by the Forest Products Laboratory. We thank FPL project leaders Carol Clausen and Sam Zelinka for their ongoing encouragement.

## References

1. NFPA 1144 (2013) Standard for reducing structure ignition hazards from wildland fires, copyright by National Fire Protection Association, 2012, 1 Batterymarch Park, Quincy, MA, 02169-7471

2. Cohen JD (2000) Preventing disaster: home ignitability in the wildland-urban interface. J For (March 2000):15–21
3. Cohen JD (2008) The wildland-urban interface fire problem: a consequence of the fire exclusion paradigm. For Hist Today Fall 20–26
4. Firewise Communities (2008) Firewise guide to landscape and construction, FWC-200-08-PH, copyright by National Fire Protection Association, 2012, 1 Batterymarch Park, Quincy, MA, 02169-7471
5. Nader G, Nakamura G, DeLasaux MD, Quarles S, Valachovic Y (2007) Home landscaping for fire, UC-ANR-Publication 8228, copyright by The Regents of the University of California, 2007, Division of Agriculture and Natural Resources
6. IWUIC (2011) 2012 International Wildland-Urban Interface Code, copyright by International Code Council, Inc., 4051 West Flossmoor Road, Country Club Hills, IL, 60478
7. Babrauskas VB (2003) Chapter 13. Special topics in ignition handbook, pp 629–631, copyright by Vytenis Babrauskas, Published by Fire Science Publishers, Issaquah, WA 98027. ISBN 0-9728111-3-3
8. Ellis P, Sullivan A (2004) The significance of suburban fuels, final CSIRO client report 1471 for Fire Management Unit Department of Urban Services ACT Government, CSIRO Contract No. FFP 04/144
9. Howard RA, North DW, Offensend FL, Charles N. Smart (1973) Decision analysis of fire protection strategy for the santa Monica mountains: an initial assessment. SRI Project MSU-2275, Stanford Research Institute, Menlo Park, CA
10. Foote EID (1994) Structure survival on the 1990 Santa Barbara'' Paint'' fire: a retrospective study of urban-wildland interface fire hazard mitigation factors. M.S. Thesis, University of California, Berkeley
11. Tran HC, Cohen JD, Chase RA (1992) Modeling ignition of structures in wildland/urban interface fires. In: Proceedings of 1st intl fire and materials conference; 1992 September 24–25; Arlington, VA; 1992: pp 253–262
12. Manzello SL, Foote EID (2014) Characterizing firebrand exposure from wildland-urban interface (WUI) fires: results from the 2007 angora fire. Fire Technol 50:105–124
13. Mutch RW, Rogers MJ, Stephens SL, Gill AM (2011) Protecting lives and property in the wildland–urban interface: communities in Montana and southern California adopt Australian paradigm. Fire Technol 47(2):357–377
14. Caton SE, Gorham DJ, Zhou A (2016) Review of pathways for building fire spread in the wildland urban interface part i: exposure conditions. Fire Technol. doi:10.1007/s10694-016-0589-z
15. McPherson G, Xiao Q, Purohit J, Dietenberger M, Boardman CCR, Simpson J, Peper P (2014) ecoSmart landscapes: a versatile SaaS platform for green infrastructure applications in urban environments. International Environmental Modelling and Software Society (iEMSs), 7th International congress on environmental modelling and software, San Diego, CA, USA
16. Babrauskas V (2008) Section 3, chapter 1. Heat release rates in the SFPE handbook of fire protection engineering, 4th edn, pp 3–34, 35
17. Tien CL, Lee KY, Stretton AJ (2008) Section 1, radiation heat transfer. In: The SFPE handbook of fire protection engineering, 4th edn, pp 1–83, 84
18. Dayan A, Tien CL (1974) Radiant heating from a cylindrical fire column. Combust Sci Technol 9(1974):41–47
19. Heskestad G (2008) Section 2, Chap. 1, fire plumes, flame height, and air entrainment. In: The SFPE Handbook of Fire Protection Engineering, 4th edn, pp 2–4

20. Quintiere JG, Grove BS (1998) A unified analysis for fire plumes, 27th symposium (international) on combustion. The Combustion Institute, pp 2757–2766
21. Tewarson A (2008) Section 3, chapter 4, generation of heat and chemical compounds in fires, Table 3-4.11. In: The SFPE handbook of fire protection engineering, 4th edn., pp 3–78
22. Tewarson A (2004) Combustion efficiency and its radiative component. Fire Saf J 39(2004):131–141
23. Chatterjee P, de Ris JL, Wang Y, Dorofeev SB (2011) A model for soot radiation in buoyant diffusion flames. Proc Combust Inst 33(2011):2665–2671
24. Wen JX, Kang K, Donchev T, Karwatzki JM (2007) Validation of FDS for the prediction of medium-scale pool fires. Fire Saf J 42(2007):127–138
25. Dupuy JL, Vachet P, Marechal J, Melendez J, de Castro AJ (2007) Thermal infrared emission-transmission measurements in flames from a cylindrical forest fuel burner. Int J Wildland Fire 16(2007):324–340
26. Adiga KC, Ramaker DE, Tatem PA, Williams FW (1989) Modeling pool-like gas flames of propane. Fire Saf J 14(1989):241–250
27. Dupuy JL, Marechal J, Morvan D (2003) Fires from a cylindrical forest fuel burner: combustion dynamics and flame properties. Combust Flame 135(2003):65–76
28. Agueda A, Pastor E, Perez Y, Planas E (2010) Experimental study of the emissivity of flames resulting from the combustion of forest fuels. Int J Therm Sci 49(2010):543–554
29. Dietenberger MA, Grexa O (2004) Ignitability of materials in transitional heating regimes. Wood & fire safety: proceedings, 5th international scientific conference, April 18–22, 2004. Slovak Republic. [Svolen, Slovakia]: Faculty of Wood Sciences and Technology, Technical University of Zvolen, 2004, pp 31–41
30. Dietenberger MA, Boardman CR (2013) HRR upgrade to mass loss calorimeter and modified Schlyter test for FR Wood. In: Proceedings of the fire and materials 2013 conference held at the Hyatt Hotel Fisherman's Wharf Hotel, San Francisco, California, USA 28–30 January 2013, pp 251–263